AD-A154 303 EXPERIMENTS IN PLASMA INITIATION AND LASER ABSORPTION IN FLOWING GASES..(U) ILLINOIS UNIV AT URBANA DEPT OF MECHANICAL AND INDUSTRIAL ENG.. H KRIER ET AL. 1/1

UNCLASSIFIED 01 APR 85 UILU-ENG-85-4004 AFOSR-TR-85-0452 F/G 20/9 NL

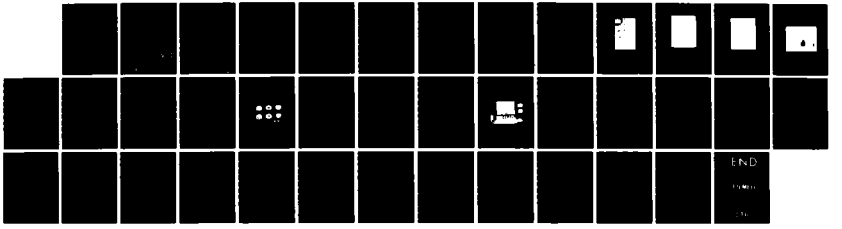

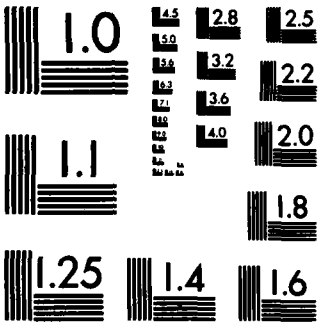


MICROCOPY RESOLUTION TEST CHART
NATIONAL BUREAU OF STANDARDS-1963-A

DEPARTMENT OF MECHANICAL
AND INDUSTRIAL ENGINEERING
UNIVERSITY OF ILLINOIS AT URBANA-CHAMPAIGN
URBANA, IL 61801



Technical Report UILU ENG-85-4004

# EXPERIMENTS IN PLASMA INITIATION AND LASER ABSORPTION IN FLOWING GASES

Annual Technical Report

AFOSR Grant No. 83-0041



Approved for public release;
distribution unlimited.

April 1, 1985

ANNUAL TECHNICAL REPORT

No. UILU-ENG-85-4004

For Research Supported by

AFOSR Grant No. 83-0041

for period 1/15/84 to 1/15/85

-entitled-

# EXPERIMENTS IN PLASMA INITIATION AND LASER ABSORPTION IN FLOWING GASES

prepared by

Herman Krier[1] and Jyoti Mazumder[1]
Ronald J. Glumb[2], Terrence D. Bender[3], and Todd J. Rockstroh[3]

Department of Mechanical and Industrial Engineering
University of Illinois at Urbana-Champaign
144 MEB; 1206 W. Green St., Urbana, IL 61801

work supported by

Air Force Office of Scientific Research/NA
Dr. Leonard H. Caveny, Program Manager



(1) Co-Principal Investigators
(2) ONR Fellow, Graduate Research Assistant
(3) Graduate Research Assistants

## REPORT DOCUMENTATION PAGE

| | |
|---|---|
| 1a. REPORT SECURITY CLASSIFICATION: UNCLASSIFIED | 1b. RESTRICTIVE MARKINGS: None |
| 2a. SECURITY CLASSIFICATION AUTHORITY | 3. DISTRIBUTION/AVAILABILITY OF REPORT: Approved for Public Release; Distribution Unlimited |
| 2b. DECLASSIFICATION/DOWNGRADING SCHEDULE | |
| 4. PERFORMING ORGANIZATION REPORT NUMBER(S): AFOSR - An. Rep. # 85-01 | 5. MONITORING ORGANIZATION REPORT NUMBER(S): AFOSR-TR- 85-0452 |
| 6a. NAME OF PERFORMING ORGANIZATION: University of Illinois at Urbana-Champaign; 6b. OFFICE SYMBOL (If applicable): UIUC | 7a. NAME OF MONITORING ORGANIZATION: Air Force Office of Scientific Research |
| 6c. ADDRESS (City, State and ZIP Code): Dept. of Mechanical & Indust. Engineering, 144 MEB; 1206 W. Green St., Urbana, IL 61801 | 7b. ADDRESS (City, State and ZIP Code): AFOSR/NA; Bolling AFB, Bldg. 410, Washington, DC 20332 - 6448 |
| 8a. NAME OF FUNDING/SPONSORING ORGANIZATION: AFOSR; 8b. OFFICE SYMBOL (If applicable): NA | 9. PROCUREMENT INSTRUMENT IDENTIFICATION NUMBER: Grant AFOSR - 83 - 0041 |
| 8c. ADDRESS (City, State and ZIP Code): Attn: Dr. Leonard H. Caveny, Bolling AFB; Bdlg. 410, Washington, DC 20332 - 6449 | 10. SOURCE OF FUNDING NOS. |

| PROGRAM ELEMENT NO. | PROJECT NO. | TASK NO. | WORK UNIT NO. |
|---|---|---|---|
| 61102F | 2308 | A1 | - |

11. TITLE (Include Security Classification): Experiments in Plasma Initiation and Laser Absorption in Flowing Gases

12. PERSONAL AUTHOR(S): HERMAN KRIER, J. MAZUMDER, R. J. GLUMB, T. D. BENDER, T. J. ROCKSTROH

| 13a. TYPE OF REPORT | 13b. TIME COVERED | 14. DATE OF REPORT (Yr., Mo., Day) | 15. PAGE COUNT |
|---|---|---|---|
| Annual | FROM 1/15/84 TO 1/15/85 | April 1, 1985 | 35 |

16. SUPPLEMENTARY NOTATION: This report represents the annual report for work done in the second year of a research program dealing with plasma initiation and beamed energy propulsion.

| 17. COSATI CODES | | |
|---|---|---|
| FIELD | GROUP | SUB. GR. |
| | | |
| | | |

18. SUBJECT TERMS (Continue on reverse if necessary and identify by block number): BEAMED ENERGY PROPULSION, ABSORPTION OF LASER ENERGY IN GASES

19. ABSTRACT (Continue on reverse if necessary and identify by block number)

This report summarizes the preliminary results of experiments designed to characterize the thermal and gasdynamic behavior of laser-sustained plasmas in flowing argon. Calorimetric measurements of global absorption have been made over a range of laser power and pressure. Temperature field mappings yield preliminary estimates of thermal gas energy and radiative losses. An infrared imaging system has been used to study plasma properties as a function of power and flow rate. Spectroscopic and laser-induced fluorescence diagnostic systems, now being installed, are highlighted. Physical implications of the data are discussed, and results of a 2-D heat addition model are presented.

*Original contains color plates: All DTIC reproductions will be in black and white*

| 20. DISTRIBUTION/AVAILABILITY OF ABSTRACT | 21. ABSTRACT SECURITY CLASSIFICATION |
|---|---|
| UNCLASSIFIED/UNLIMITED ☒ SAME AS RPT. ☐ DTIC USERS ☐ | UNCLASSIFIED |

| 22a. NAME OF RESPONSIBLE INDIVIDUAL | 22b. TELEPHONE NUMBER (Include Area Code) | 22c. OFFICE SYMBOL |
|---|---|---|
| Dr. Leonard H. Caveny | 202-767-4937 | AFOSR |

DD FORM 1473, 83 APR — EDITION OF 1 JAN 73 IS OBSOLETE.

## Scientific Issues Addressed

Continuous wave (CW) laser propulsion, as envisioned for orbit-raising purposes, makes use of a focused high power laser to create and sustain a high temperature plasma in a flowing medium. Energy is then transferred to the working gas through interaction with the plasma. The key to understanding and evaluating this form of laser propulsion lies in a solid understanding of the physics of the plasma, and the gasdynamic interactions of the plasma with the gas.

### Physics of the Problem

The laser-sustained plasma is usually initiated by focusing a high power laser onto a metallic target. At the high energy densities available at the focus, the metallic surface first vaporizes, then the neutral atoms undergo multiphoton absorption. Due to the low ionization potential of the first bound electron of these atoms (typically less than 5 eV), ionization can occur before deexcitational collisions take place. In gases such as argon, the first ionization potential is many times higher than for metals. Thus ionizing pure argon without a target would require many more photon absorptions per second, and requires a much higher laser intensity.

Once the metal atoms have ionized and free electrons are present, another type of absorption process begins. This is inverse Brehmsstrahlung absorption, a process in which a free electron, when interacting with a nearby ion or neutral, absorbs a photon. These free electrons are now heated to very high temperatures, and as they collide with neutral atoms, enough energy is transferred to produce ionization of additional electrons. This chain reaction, known as an electron cascade, continues until the metal vapor is highly ionized and the absorption is dominated by the IB process.

The vaporization/ionization of the metallic target occurs almost instantaneously, producing a cloud of high-temperature highly ionized metal vapor above the target. At this point, the metal vapor begins heating the surrounding argon through radiation and conduction. This heating quickly causes ionization of the neutral argon atoms, allowing argon to begin absorbing on its own through the IB absorption process. Once this has occurred, typically in a fraction of a second, the target may be removed and the argon plasma is sustained in the convergant section of the laser beam.

The laser-sustained plasma exhibits many of the phenomena of gasdynamic waves. In particular, it will move up a converging beam at a velocity that is a function of laser intensity. This is because the hot plasma will radiatively heat the cooler gas that is upstream and cause the plasma as a whole to move upstream. The plasma becomes stationary when the incoming velocity of the gas just matches the wave velocity of the plasma. Typically, the plasma is a highly stable phenomenon, since it will tend to seek out a location in the converging beam where the intensity-dependent wave velocity produces this match. This position will also correspond to the location where radiative losses from the plasma balance the absorbed energy from the laser.

As the laser power is reduced (or as the flow velocity is increased), the plasma is forced closer and closer to the focal volume. Once this point is reached, the plasma can retreat no further, since it cannot be stably maintained in the diverging section of the beam. If the power is reduced any further, the plasma will immediately extinguish, and will not reform unless the target is reinserted.

Objectives and Methods

Much of the physics of the laser-sustained plasma is not yet completely understood. Such basic factors as global and local absorption, temperature distributions, and gasdynamic interactions have yet to be measured in detail. The only way to gain a full understanding of the plasma is by accurately mapping its properties (both local and global) throughout the flowfield, and comparing the results to theoretical assumptions of the physics. The objective of the current work at the University of Illinois is to provide these fundamental measurements so that the operating physical mechanisms may be clearly defined.

The primary and most complex goal is the complete mapping of the temperature field within and near the plasma. Such mapping provides important information on local absorption behavior, radiative and thermal heat transfer, and fluid mechanics. Because of the extreme temperature ranges involved, different techniques are used in different areas.

In the plasma core, spectroscopic relative line intensity techniques are being used for electron temperature, and Stark broadening for number density. The flexibility of our system also permits verification of the assumptions of LTE and optical thickness, and will allow precise spatial measurements of plasma dimensions.

In the cooler regions far downstream, thermocouple probes are used. And at intermediate temperatures, an LIF system will be employed. The LIF system will also be useful in mapping the transient flowfield throughout the entire downstream region. All of these measurements are being made at varying pressure, laser power, and flow velocity (including blowout and extinguishment limits) so as to determine dependencies.

In conjunction with these temperature measurements, an IR thermography system is being used for qualitative studies of plasma position and size at various combinations of power and flow rate.

Another objective is a complete measurement of global absorption as a function of laser power, pressure, optical geometry, flow rate, and seed concentration. Such data is invaluable in checking basic assumptions about the absorption coefficient, and in making estimates of the overall thermal efficiency of the system.

Finally, we are now engaged in developing a two-dimensional model of laser heat addition to flowing argon. The code uses real gas properties and a two-dimensional geometry. A radiation loss mechanism is now being added. The eventual goal is to compare calculated temperatures, absorption, and efficiencies with those measured in our experiments.

## Achievements of '84-'85 Research Program

During the second year of funded research, the following items were completed:

- PIFC plasma flow chamber completed final assembly and was successfully pressure tested (5/84)
- First initiation of plasmas in air (6/84)
- Calibration of high-flux calorimeter (7/84)
- Spectroscopic optics designed and installed (9/84)
- Preliminary tests of OMA 2 spectroscopic system (10/84)
- First initiation of plasmas in flowing argon (11/84)
- Calorimeter data taken at various combinations of laser power, optical f/#, and gas pressure (11/84)

- Purchase of excimer laser system for LIF studies (11/84)
- High-speed films of chamber flow patterns taken using smoke (12/84)
- Fluke computer system programmed to record data and control experiments (1/85)
- Heat addition model used to predict plasma size and location at various laser powers and flow velocities (1/85)
- IR camera system used to record images of filtered plasma at various combinations of laser power and flow velocity (2/85)
- Thermocouple measurement system installed and tested (2/85)
- Preliminary TC scans of areas around plasma completed (3/85)
- Preliminary estimates of thermal gas energies and radiative losses based on isotherm plots of TC data (3/85)
- OMA 2 and 3 systems debugged and repaired (2/85)
- First OMA-3 temperature measurements of argon plasmas attempted (3/85)
- Emission spectra of argon plasma recorded at 400 - 600 nm (3/85)
- Model extended to include radiative losses in argon (3/85)

Several of these accomplishments are highlighted in the photographs of Figures 1 - 4. In the following sections, we present our preliminary data, along with possible physical interpretations of what is happening in the laser-sustained plasma. The techniques and equipment used are also described.

## Calorimeter Data

Preliminary measurements of global plasma absorption have been completed. This data was taken as a function of laser power, gas pressure, and optical geometry so as to reveal important physical trends. Such absorption data at these power levels has never before been presented.

The data, plotted in Figure 5, indicates strong laser energy absorption by argon, approaching 80% at higher powers. The argon absorption is consider-

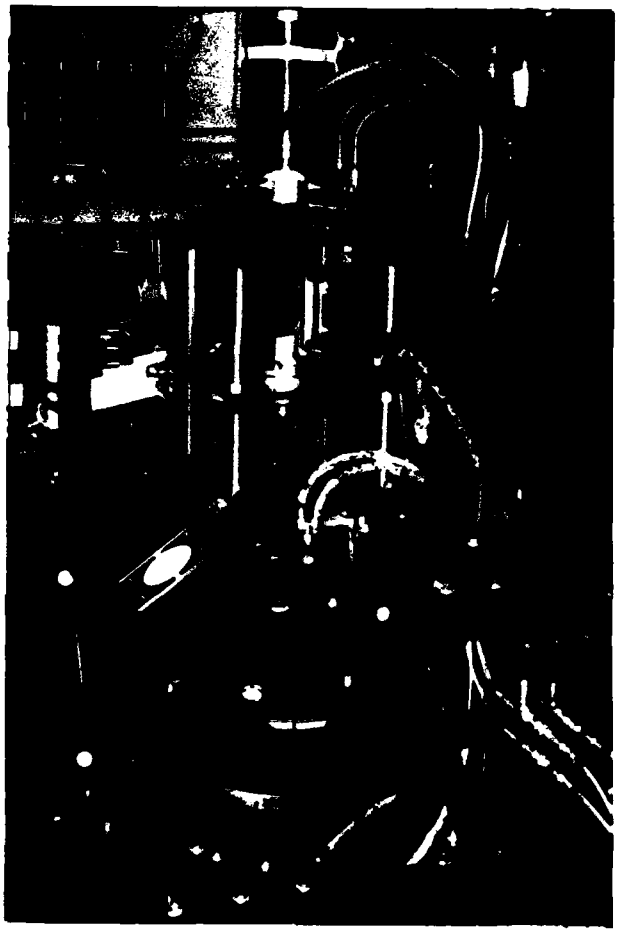

Figure 1 Flow Chamber and Laser Optics Mounted on Mobile Test Stand. High-Flux Calorimeter is at the Top of the Photo.

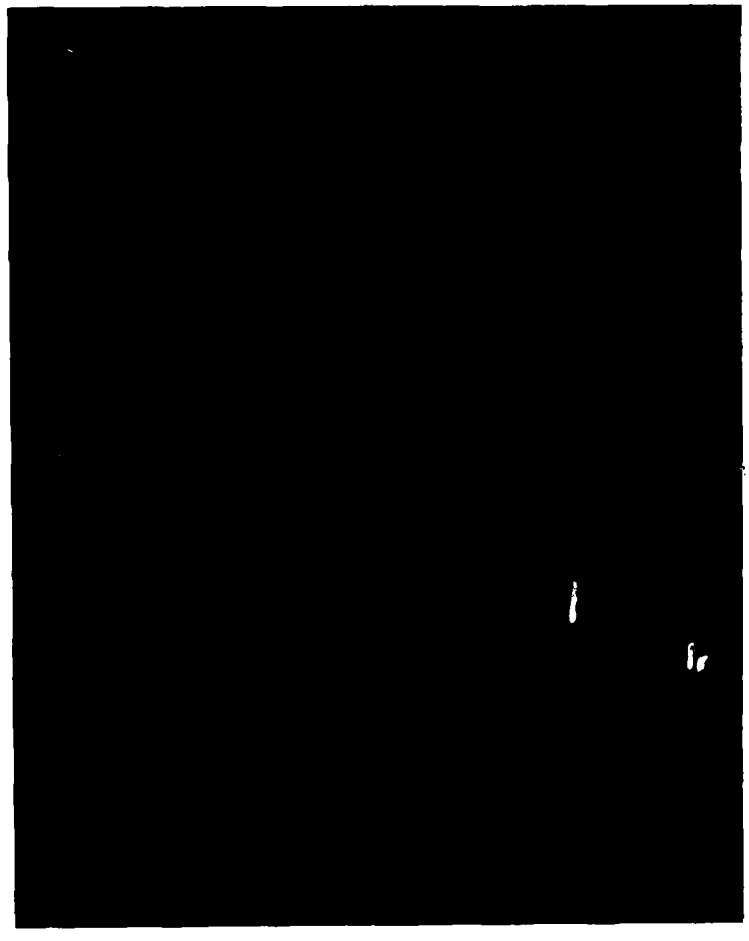

Figure 2 Optical Path of Variable f Number Optical System.

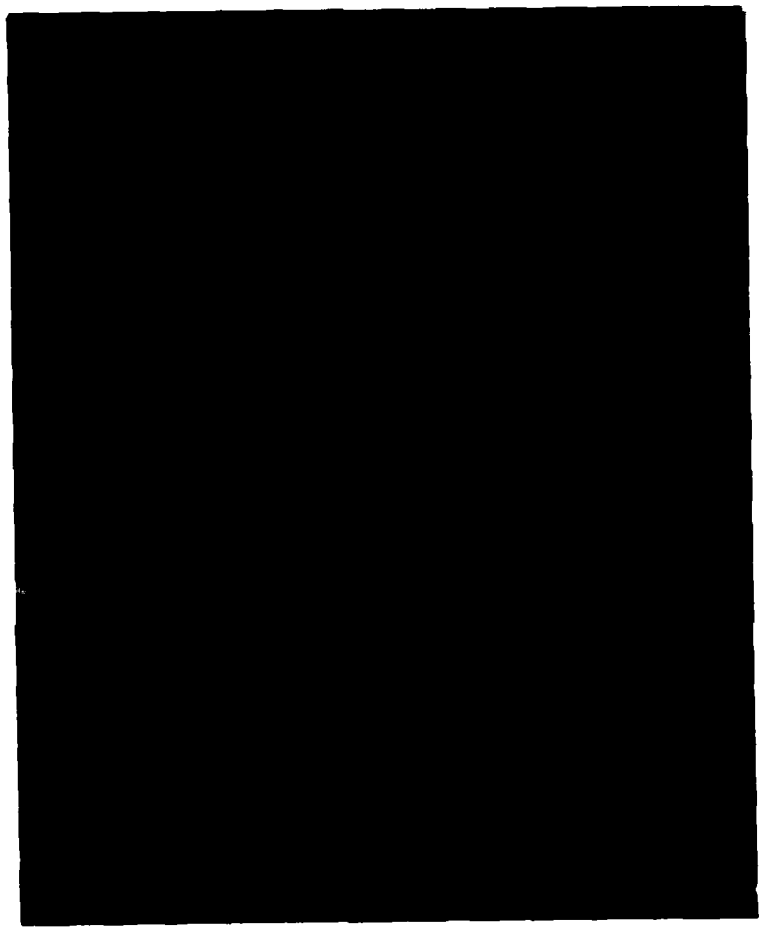

Figure 3 Focal Volume Inside Chamber at f/3.0. The Thermocouple Carriage is Visible Above the Focus.

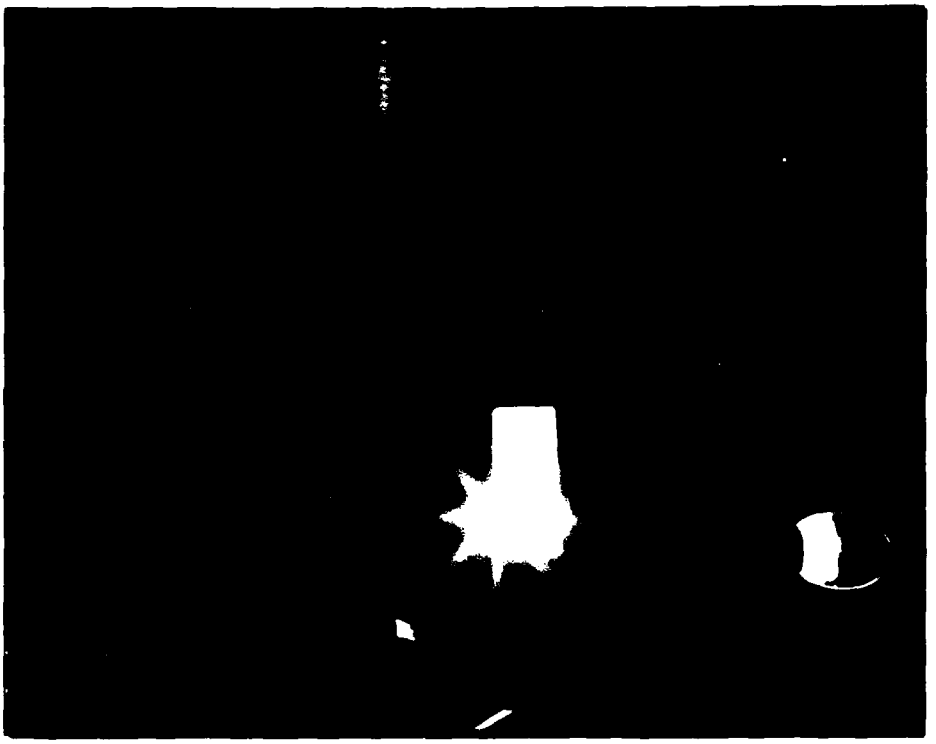

Figure 4 Laser-Sustained Plasma in Air; Calorimeter Removed for Clarity. Note the Back-Reflection Through the Laser Optics at Right.

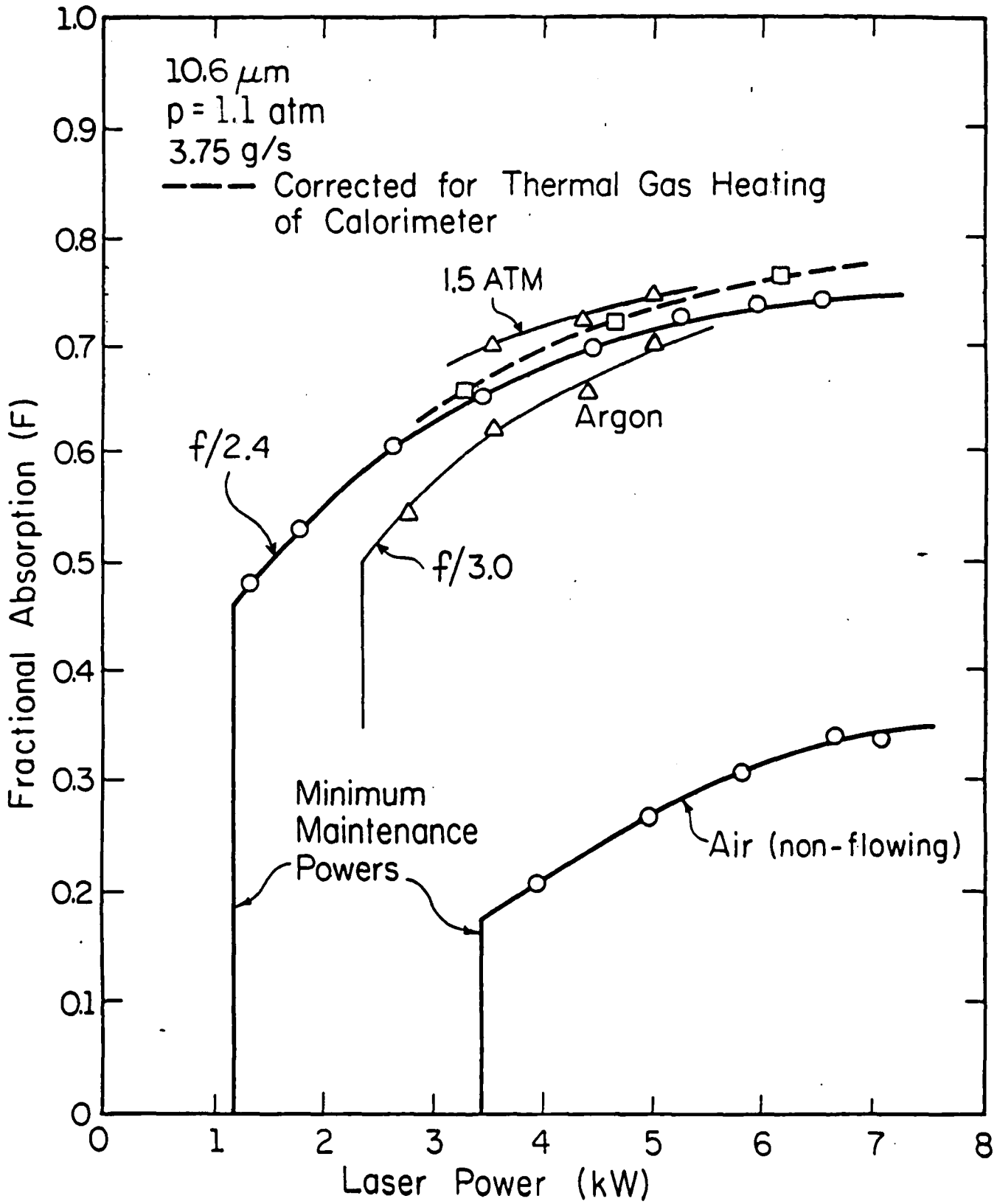


Figure 5 Calorimeter Data for Argon and Air Plotted versus Laser Power, f Number, and Pressure.

ably stronger than that of air, due mainly to its higher absorption coefficient. The absorption coefficient of air is degraded by the presence of extraneous species with larger electron collisional cross sections. These tend to deexcite free electrons and lower electron temperature, reducing inverse Brehmsstrahlung absorption, the dominant absorption mechanism.

The data also shows a tendency for global absorption to rise with laser power. This is most likely a geometric effect. Total absorption depends both on absorption coefficient and on plasma size. Plasma size is an eigenvalue solution of the steady state energy balance equations (see Fig. 6), producing a finite plasma size for a given laser power and flow conditions. As laser power increases, the plasma size and therefore the absorption length grow, causing a net increase in global absorption.

The data also suggests asymptotic behavior at high power (see Fig. 6b). This can be explained physically. As laser power increases, the plasma grows until it reaches a point where increasing radiative losses from the enlarged surface area offset any increases in power, preventing further growth in absorption length. The upper limit should depend largely on beam geometry and radiative behavior.

The data for argon at 1.5 atm is still tentative, but suggests that absorption increases with pressure. This would be as expected, since the IB absorption coefficient is a strong function of number density and therefore of gas pressure.

A comparison between two optical geometries (f/2.4 and f/3.0) was also made. As expected, the more tightly focused f/2.4 system produces slightly higher absorption readings. This is due primarily to the smaller focal volume that is possible with this system.

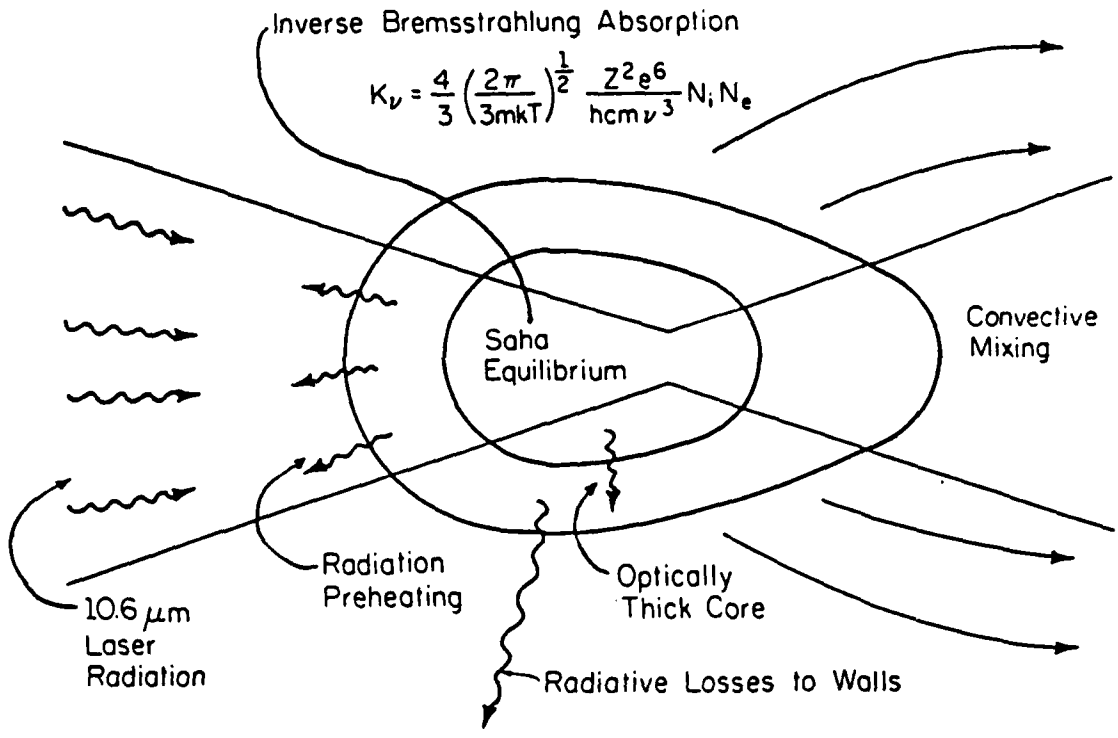


Fig. 6a Physical mechanisms affecting the energy balance of the LSP. The plasma stabilizes at a point in the focused beam where the absorbed power equals all loss mechanisms.

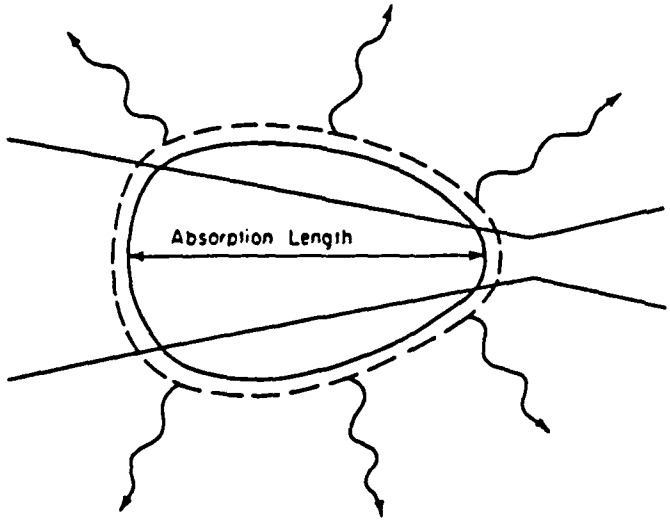


Fig 6b Increased radiative losses due to larger surface area offset increases in laser power and fix an upper limit to plasma size and global absorption fraction.

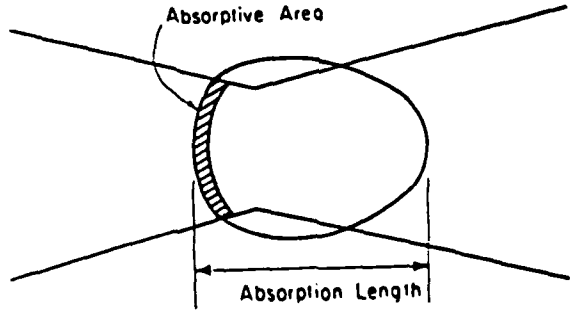


Fig 6c Near plasma extinguishment, absorption area and length are fixed by the focal volume. Thus, minimum maintenance power is a function of absorption coefficient only.

Minimum maintenance powers for the two systems are also shown on the figure. The reason for the difference is related to the plasma's behavior near extinguishment (see Figure 6c). As laser power is reduced, the plasma is held very near the focal volume, where absorptive area is highly dependent on the f number. (The higher minimum values for air are again caused by its smaller absorption coefficient.)

The dashed line above the argon data represents an analytic correction for the heated gas that becomes trapped in our calorimeter; it is based on thermocouple readings taken inside the calorimeter cone. Actual measurements of the correction factor are now being made using NaCl windows placed in front of the calorimeter.

Infrared Thermography Data

In order to qualitatively map the shape and location of the plasma in real time, we have made use of an infrared thermography system sensitive to 8-12 μm radiation. Though direct temperature measurements of the plasma core are not feasible at this time, the system does produce detailed false-color qualitative temperature mappings of this region. Figure 7 presents several such images, taken at various laser powers and at two flow velocities.

Several important trends are noticable. First, as laser power falls, the plasma becomes cooler and smaller, and moves closer to the focus point. Increasing the flow velocity produces much the same effect. Note also that in both cases, the plasma core appears to move past the focus point before extinguishing.

The circular IR images contrast with the teardrop-shaped plasmas that can be seen in the visible spectrum. We believe that this is the result of

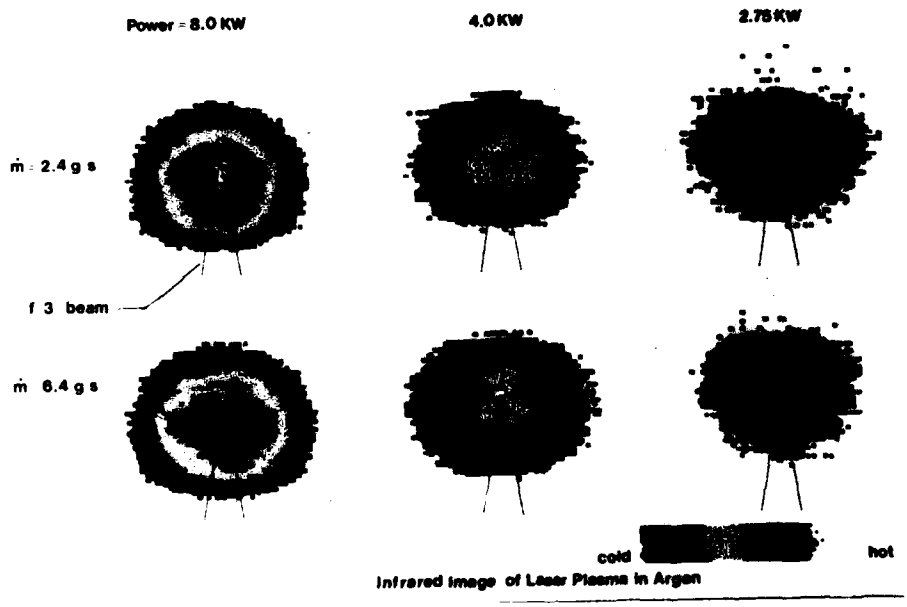


Figure 7 Infrared Images of Argon Plasmas.

increased optical thickness at the longer IR wavelength, since the re-absorption coefficient is proportional to the cube of the emission wavelength. Thermal blooming of the filter is also a possibility, one which is now being examined.

Eventually, it is our hope that the IR system may be used for approximate quantitative temperature measurements of the plasma core. This may be possible by comparing the IR images (after Abel inversion) to temperature data produced using the OMA spectrograph. Temperature measurements of the cooler downstream region is also possible, though the gas emissivity in this area is highly dependent on gas temperature.

## Spectroscopic Temperature Measurements

Electron temperatures within the plasma core will be found by spectroscopically measuring the relative line emission intensities of argon. The instrument we are using for this purpose is an EG&G PARC Optical Multichannel Analyzer (OMA) III system. The OMA consists of a computer console, detector controller, silicon intensified target (SIT), monochromator, and collection optics. Although the OMA was first received in July 1984, numerous software and hardware problems were not fully corrected until this March, delaying data acquisition and analysis.

The system is used as shown in Figure 8. The plasma is first imaged onto the monochromator entrance slit. The monochromator then spectrally diffracts the incident light onto the two-dimensional vidicon SIT. Through computer control of the SIT, the vidicon array can be segmented into tracks which effectively divide the plasma image into independent segments horizontally spaced across the plasma. The monochromator/SIT assembly is then translated vertically, allowing rapid scans of the entire plasma.

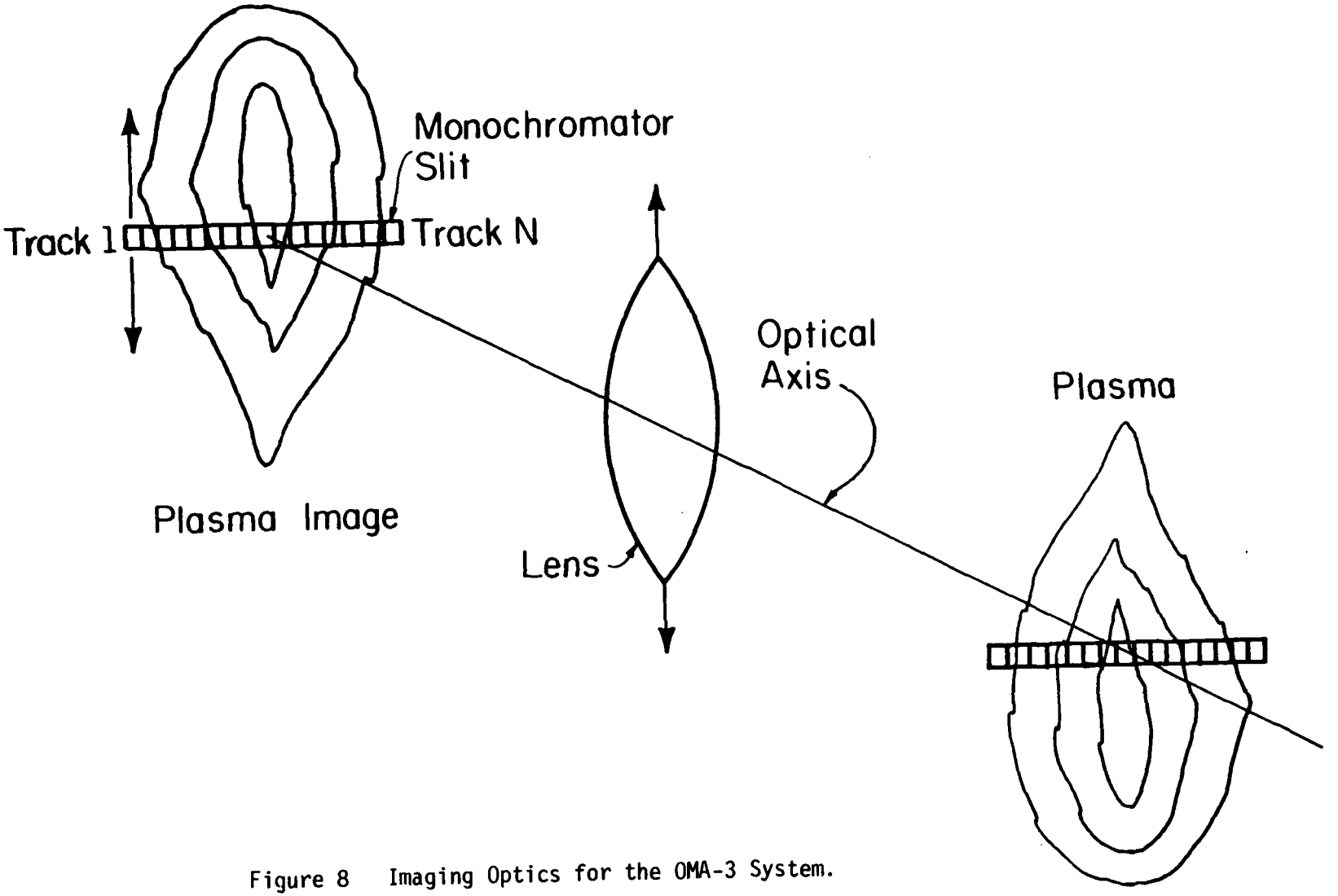


Figure 8 Imaging Optics for the OMA-3 System.

Figure 9 presents a sample data set of 15 tracks, as shown on the OMA console display. The tracks represent single points which cut horizontally across the plasma. The plot is line-of-sight intensity (vertical scale) versus wavelength (horizontal) versus position across the plasma (into the screen).

The OMA data is used to determine electron temperature via the relative line intensity technique. At each scan position, the intensities at two separate wavelengths are curve-fitted against plasma radius. Since the data is a line-of-sight integrated value, the curves will be Abel-inverted to yield radial (point) emissivities. The ratio of the emissivities at the two different wavelengths at a given plasma location is proportional to the electron temperature. If two semi-independent pairs of lines (emissivities) can be resolved to yield similar temperatures, then the OMA can be used to verify the spatial extent of local thermodynamic equilibrium (LTE) in the plasma core. The visible spectrum transitions are of interest, though there is a question of optical thickness in this region. This could reduce the signal-to-noise ratio above the continuum, but the relative value of the lines should remain largely unchanged.

The Abel inversion requires axial symmetry in the plasma, which may or may not be the case due to the characteristics of our laser optics. A computer code has been developed which fits the intensity data at a given wavelength with a cubic polynomial. The routine is restricted to positive radial dimensions by averaging the data reflected about the axis. To date the differences in symmetric points have been less than 10%.

The Abel inversion is an integration of the differential intensity curve. However, to achieve a higher S/N ratio, a dummy function is set up

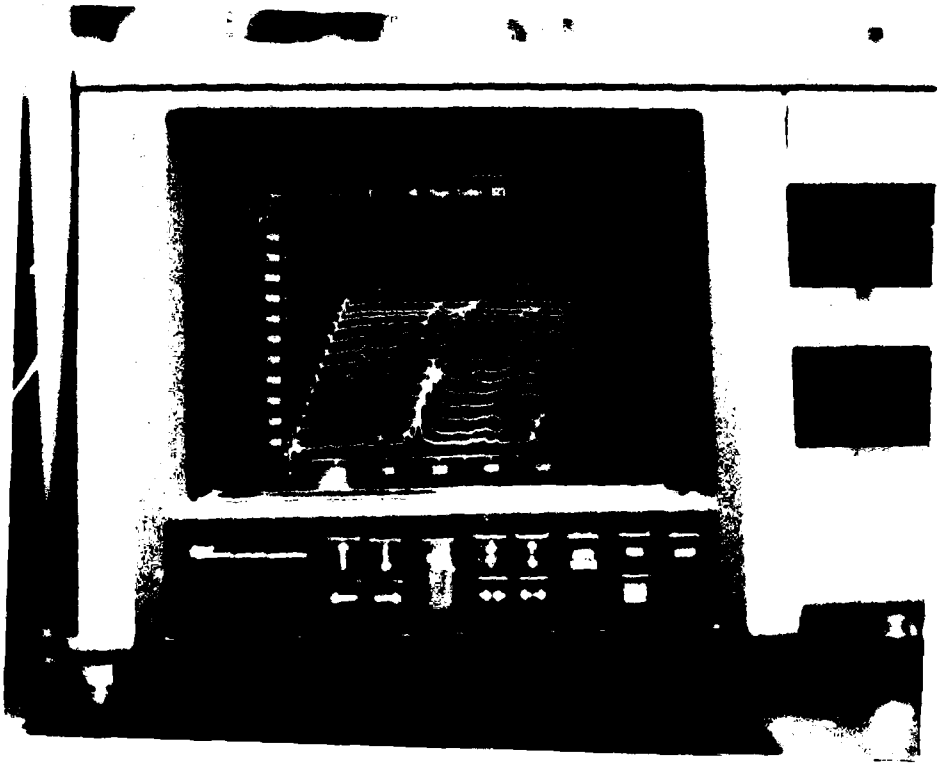

Figure 9 Spectroscopic Data on OMA-3 Display Screen. Data is for an Argon Plasma at 1.1 atm.

which is first integrated (smoothing) and then differentiated to yield radial emissivity. The asymmetry will be monitored and if necessary, asymmetrical inversion techniques will be implemented.

The OMA will also be used to measure the Stark (pressure) broadening of the $H_\beta$ (486.1 nm) line to determine the electron number density. The Stark effect should dominate other broadening effects in the pressure range of interest. The water content of commercial argon should provide a sufficient concentration of hydrogen to monitor this line. The profile can be matched to calculated and empirical data of hydrogenic lines with accuracies approaching 5%.

Once the electron temperature and number density are known, it becomes possible to calculate atomic parameters through the equilibrium relationship. It should be noted that although LTE should hold throughout the plasma core, this does not necessarily imply that the gas temperature equals the electron temperature. Since the gas temperature determines ultimate thermal efficiency, an assessment of the energy transport between electrons and heavy particles will be made.

The advantage to using this type of system is that its flexibility and the variety of techniques available make it possible to verify the LTE assumption and independently check our results. Studies of the spectral emission behavior of the plasma are also possible.

The advantage of an OMA system lies in its flexibility. Any region of the spectrum between 350 and 830 nm can be monitored to determine plasma parameters. The system has internal functions and computation capabilities useful in the preliminary reduction of data and can be interfaced to a host CPU for final data manipulation.

Thermocouple Measurements

Gas temperatures under 3000 Kelvin in the flow around the plasma were measured with Tungsten-Rhenium thermocouples. These thermocouples were mounted on a movable carriage capable of traversing the chamber length. Figure 10 shows an axial view of the carriage and the combination of thermocouple orientations used. A remotely programmed stepper motor moves the carriage to any desired location at a selectable velocity. A FLUKE 2452 MCS (measurement and control system) controls both the stepper movement and the scan rate of the thermocouples. This allows us to obtain two and even three dimensional temperature maps of the flow around the plasma.

Figure 11 is a scale view showing the region in which thermocouple measurements have been made. Notice that the laser beam intersects part of the measurement zone in this example. The radiation effect on the thermocouples across this intersection will be discussed below. The plasma core is too hot to measure with thermocouples so it was avoided. For future reference, the exhaust plane of the chamber is considered the rightmost edge of the measurement zone, downstream of the plasma.

Figure 12 is the temperature map of the measurement zone seen in Figure 11. The isotherms were constructed from a coarse grid of 320 discreet points spread evenly through the measurement zone. The temperatures along the wall are in the neighborhood of 500 K and near the plasma as high as 2600 K. Along the beam intersection with the measurement zone the temperature rises contrary to the general trend. It appears that the thermocouples are being affected by laser energy transmitted through the plasma. We are currently examining ways of shielding the TC's and/or correcting for this radiative heating.

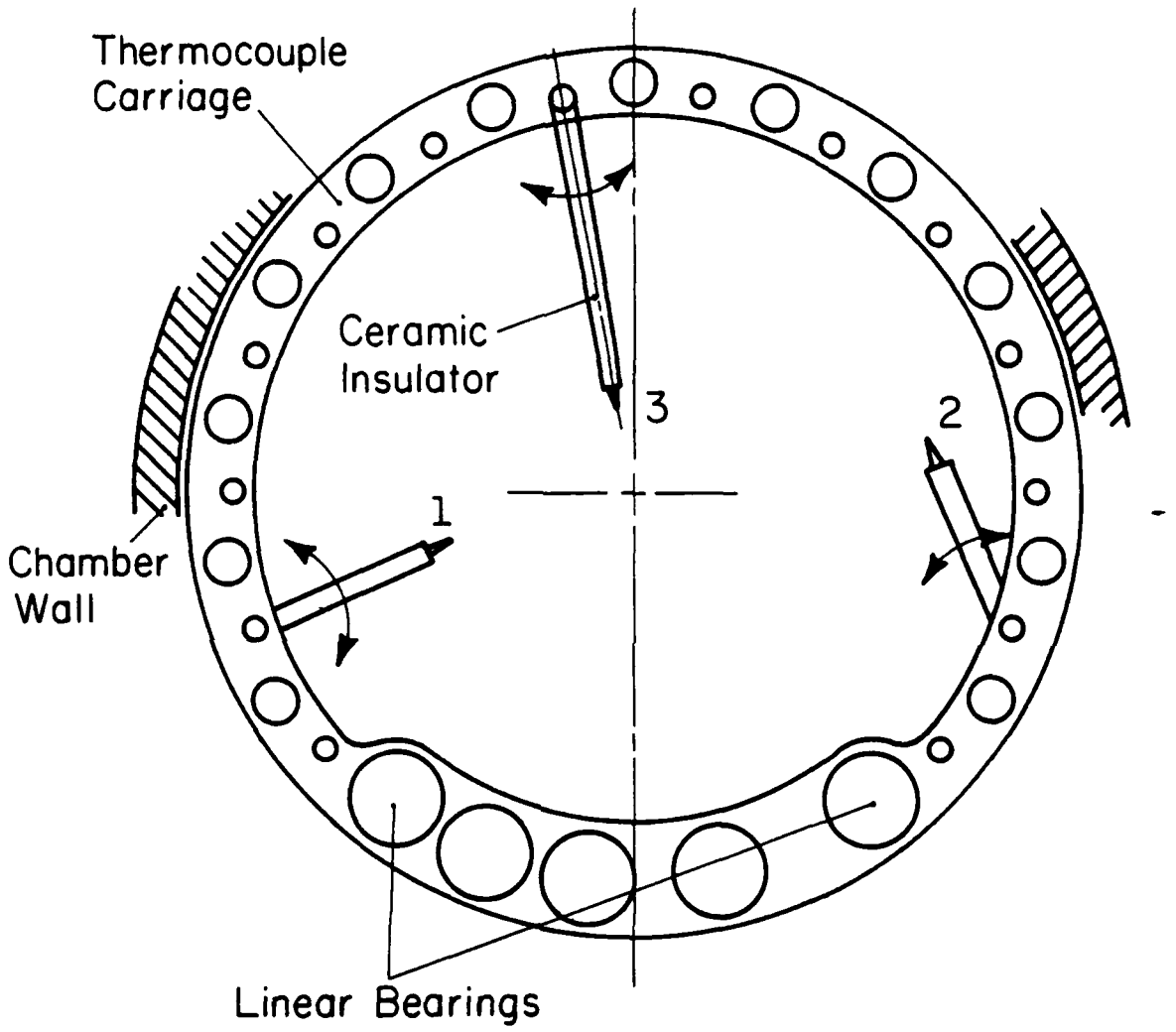


Figure 10 Thermocouples Mounted on Movable Carriage. TC's Can Be Pivoted for a Variety of Scan Configurations.

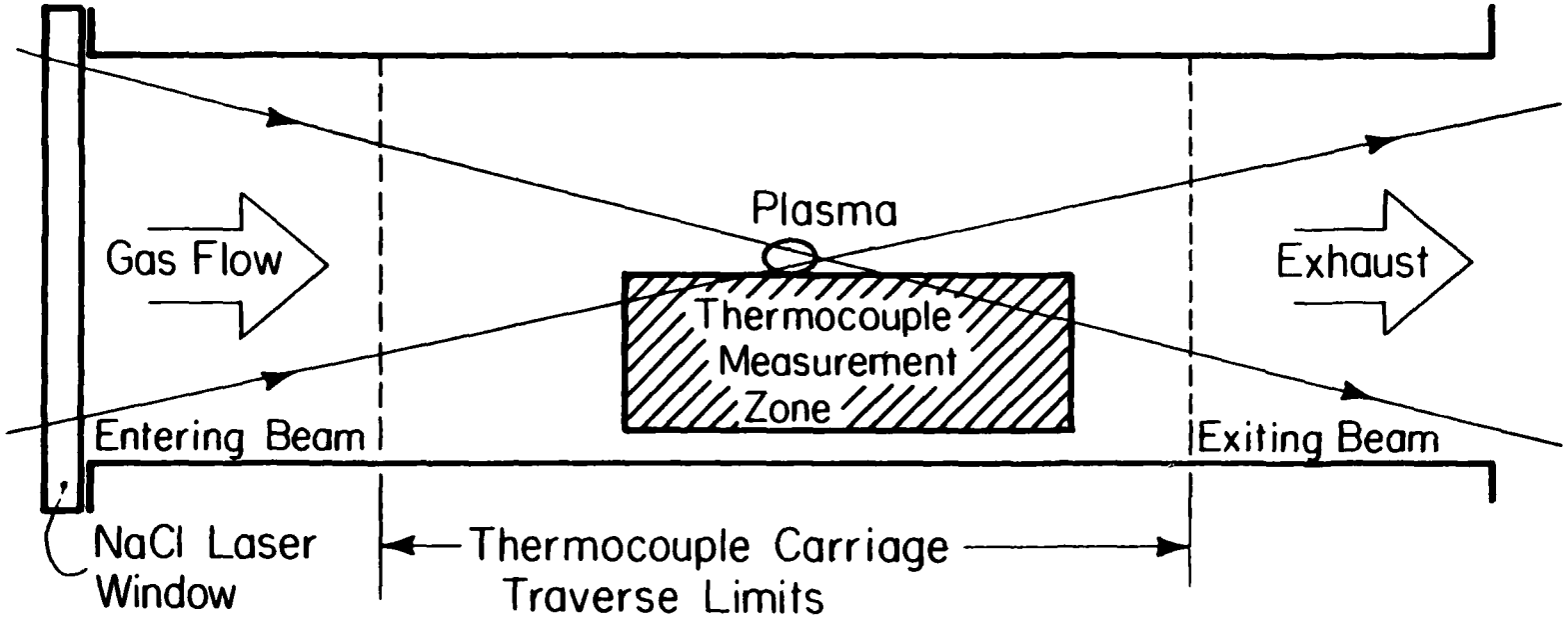


Figure 11 Area in Which Thermocouple Measurements Have Been Made.

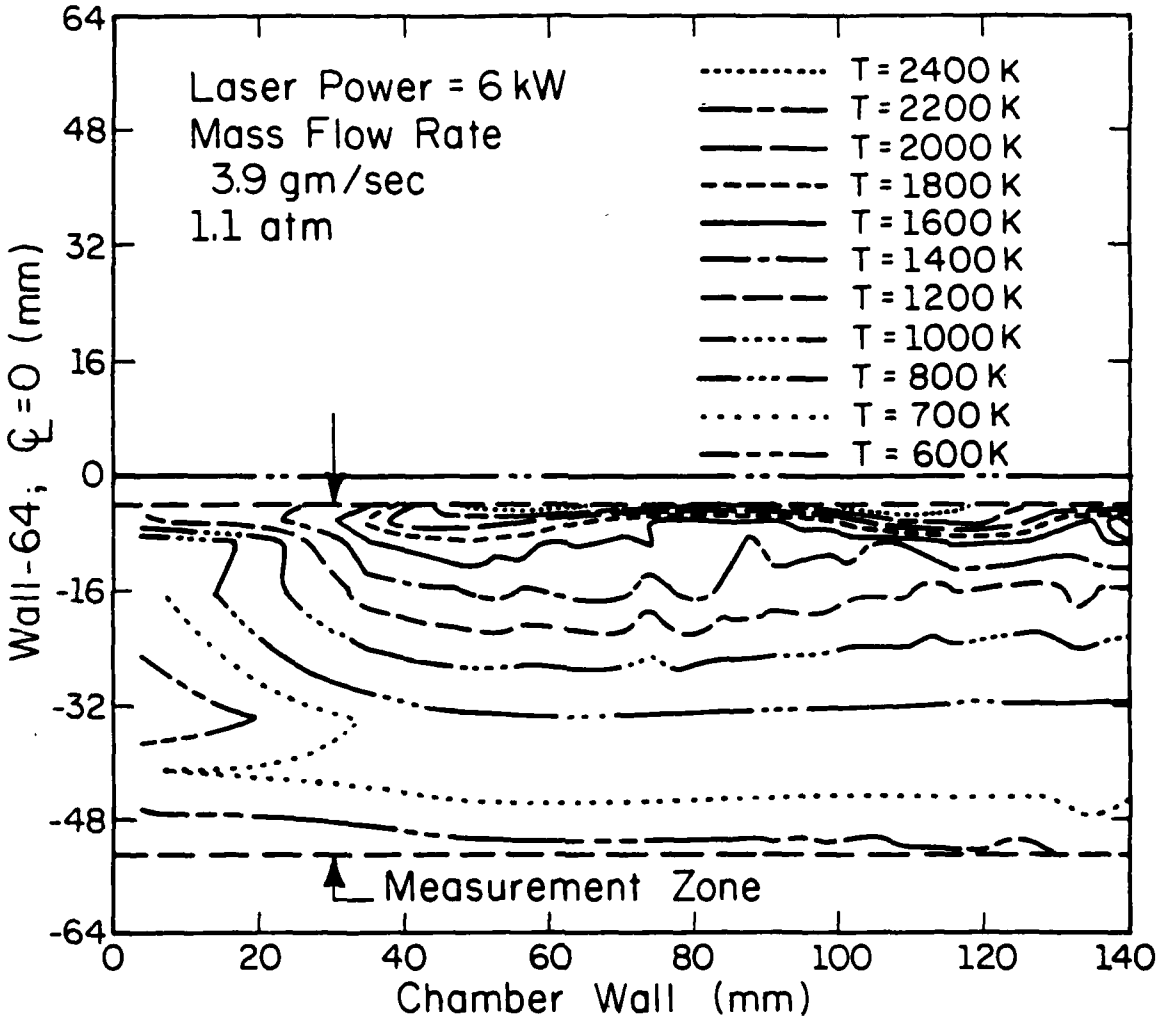


Figure 12 Temperature Isotherms Produced Using Thermocouple Scans. Hot Spots in Upper Right Caused by Transmitted Laser Heating. Disturbance at Lower Left Suggests Reversal of Flow at Walls.

The isotherms indicate the shape of the mixing layer around the plasma and the shape of the hot buoyant plume downstream. Notice the temperature contours upstream of the plasma and near the wall, where the flow appears to reverse and flows upstream. Figure 13 illustrates what is happening more clearly. The hot buoyant plume rises violently, increasing the flow velocity along the centerline far above the mean. To preserve conservation of mass, the flow along the wall must reverse. The greatest consequence is that the flow velocity and probably the mass rate of flow through the plasma is much larger than what the bulk flow rate would indicate.

The thermocouple measurements allow us to estimate the thermal efficiency of a laser-sustained plasma by estimating the exit plane enthalpy. Figure 14 indicates how this was done. The exit plane temperatures and radial position were taken from the data. Simpson's Rule was used to obtain an area averaged temperature of the exit plane. For this case, it was found to be about 849 K. The mass flow rate, laser absorption, and specific heat of Argon are also known.

The results of this analysis are illuminating. With an input power of 5.5 kW, the thermal energy of the gas was found to be 2.04 kW, 37% of the total. From the calorimeter data we know that an additional 28% of the laser energy is transmitted through the plasma and lost. The remainder of the energy ( 35%) must therefore be lost as thermal radiation to the chamber walls.

This represents the first experimental estimate of the thermal efficiency of a laser-sustained plasma. Although preliminary, the results are consistent with the estimates made by some theoretical modelers.

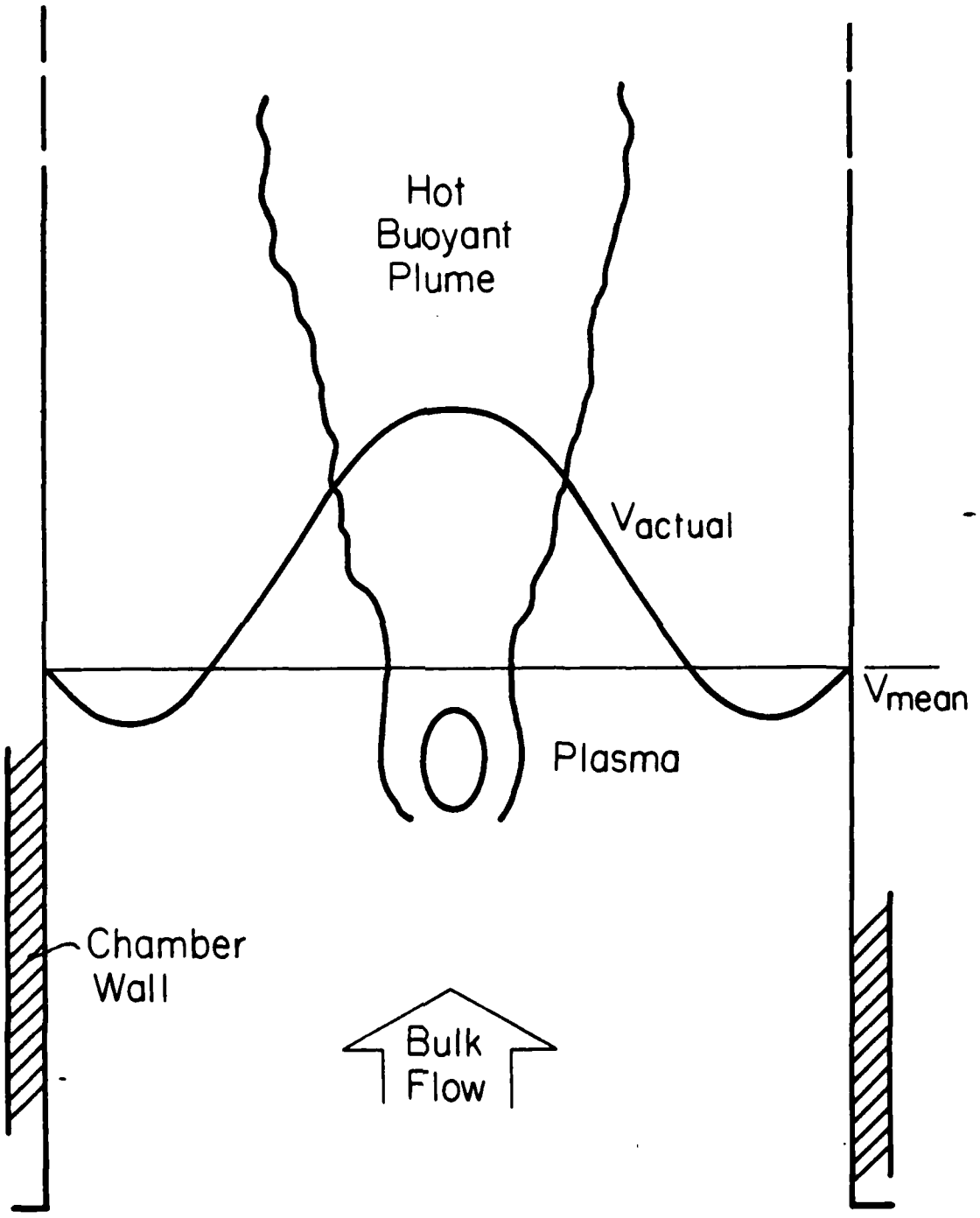


Figure 13 Estimated Velocity Profile
Based on Thermocouple Data.

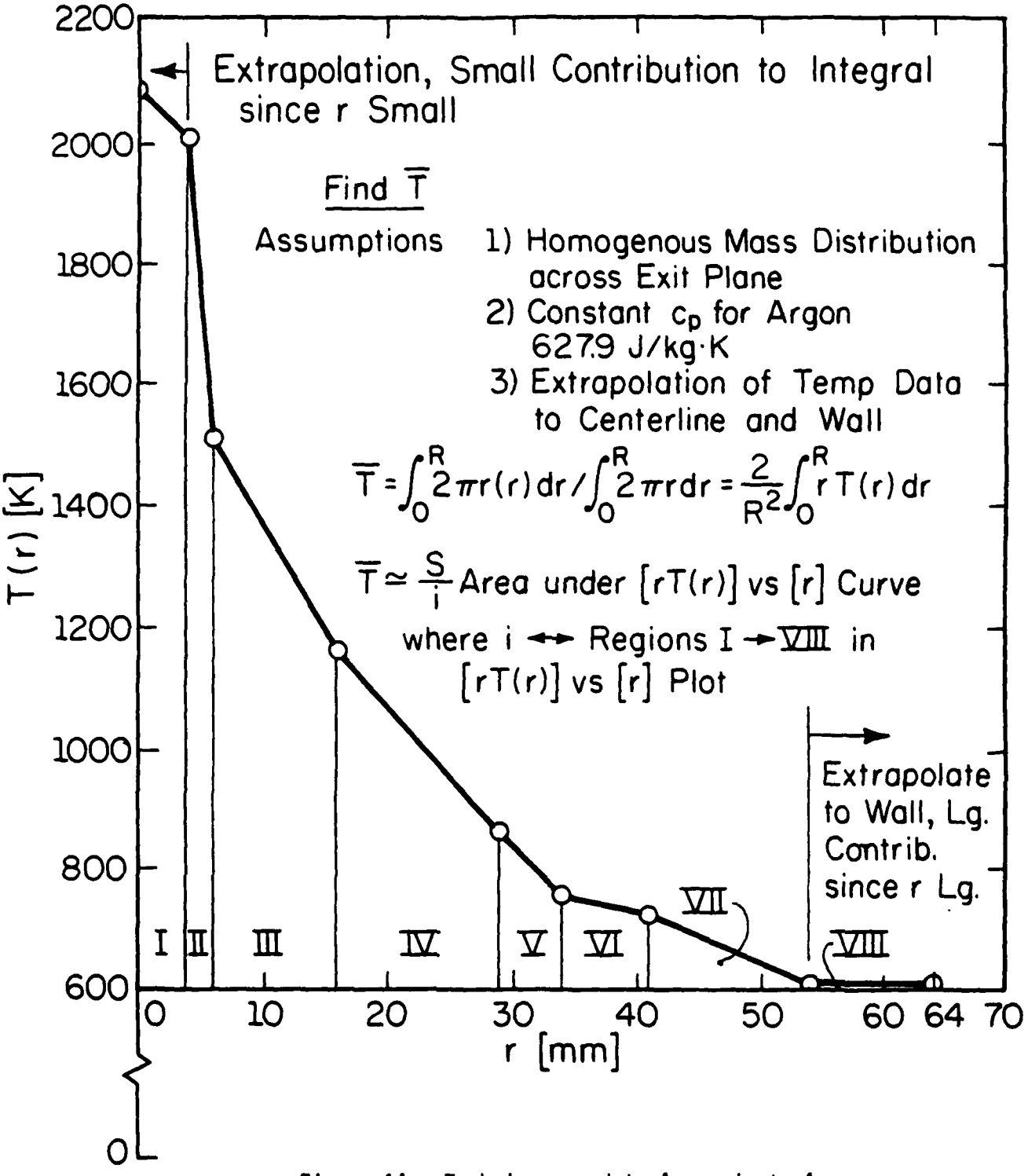


Figure 14 Technique used to Approximate Average Exit Temperature.

The analysis needs further refinement, however. The exit plane temperature should be a mass averaged value. To obtain this we intend to calculate the "mixing cup" temperature using pitot tube velocity measurements at the exit plane. This will allow us to calculate not only flow velocity, but density and thus mass flow as a function of radius.

Excimer Laser System

To aid in laser-induced fluoresence studies, we have recently purchased a Lambda Physik excimer pumped dye laser system. The dye laser is wavelength tunable through the adjustment of the resonator cavity and the dye cell. When used for LIF, the laser will be tuned to excite a specific transition in argon or a seeded material. Monitoring the fluorescent deexcitation intensity on a point by point basis yields considerable information on concentrations and/or temperatures within the flowfield. This information will be used for flow visualization in the areas downstream from the plasma, as well as for temperature measurements in the bulk gas.

The utilization of LIF requires the choice of a proper fluorescent seedant in the flow. Also, adequate shielding of the core radiation will be necessary to detect the relatively weak fluorescent signal. Neither problem is trivial, and we intend to make use of the expertise of Dr. Ron Hanson in setting up the system. Dr. Hanson is currently working in conjunction with UIUC on another proposal before AFOSR.

In addition to the LIF studies, the excimer laser system will be used for UV plasma initiation experiments. The excimer system being purchased is one of the higher power units available (100 W average), and has one of the higher pulse rates (250 pps). Using UV emission at either 193 nm (ArF) or 248 nm

(KrF), we hope to be able to both initiate and sustain a plasma in flowing argon. This presents the opportunity of measuring the wavelength dependence of plasma properties.

## Heat Addition Model

Analytical modeling of the laser-sustained plasma is an important aspect of the overall research effort. Most importantly, it offers insight into the physical processes that are taking place in and near the plasma. When analytical results are compared to experimental data, it becomes possible to determine which processes are dominant, and which tend to be unimportant. In addition, models are useful in scaling systems to higher laser powers, something which cannot as yet be done experimentally. Finally, a complete model can be used to find ways of maximizing the thermal efficiency of the system.

Until recently, the effort to model laser-sustained plasmas was incomplete. The majority of the models were one-dimensional in nature, and could not include the important geometrical dependencies encountered in the plasma. The few that did include a 2-D geometry tended to ignore the real properties of the working gas, isolating the analysis from reality. Very recently, Merkle has attempted to include two-dimensional flow and real gas properties, but results are as yet inconclusive.

The main thrust of our modeling effort is to include a 2-D geometry and real properties, but to use the restriction that the flow is one-dimensional in nature (i.e. the radial velocity component is zero). The major effect of this simplification is to make the plasmas more elongated and raise peak temperature slightly; however, the assumption should not radically affect the validity of the results. Also included in the model is a realistic radiation

loss term which uses analytically derived emission coefficients for both free-bound and free-free transitions. We also hope to eventually include a radiative transport mechanism for exchange within the gas, and to use an approximate treatment for dealing with two-dimensionality of the flowfield.

The assumptions of no radial flow and constant pressure reduce the number of equations to just one: the 2-D energy equation with conduction, convection, laser heat addition, and radiation loss. At each cell location, the energy equation is solved explicitly for temperature using a modified Gauss-Seidel overrelaxed iterative scheme.

A preliminary set of solutions for hydrogen at one atmosphere is presented in Figures 15 - 18. Figure 15 shows the effect of decreasing laser power at a flow rate of 20 cm/s, and Figure 16 shows the effect of higher flow velocities at 50 kW. In each case, note that peak temperatures are above 20,000 K and bulk exit temperatures are in the 3000 K range. As the power is lowered, or as the flow rate increases, the plasma moves closer to the focus, extinguishing as the plasma front is forced through the focus point. Figure 17 is a plot of plasma front position versus the two variables, and shows this extinguishment behavior more clearly.

Figure 18 is a comparison of a hydrogen solution to our first argon solution, both at the same laser power and mass flow rate. Note that because of the higher density of argon, the flow velocity of the argon case is about 1/20th that of the hydrogen case. Because of argon's much lower specific heat, the argon plasma is considerably larger, though due to a lower-temperature peak in absorption coefficient, the peak temperatures are somewhat lower (under 20,000 K).

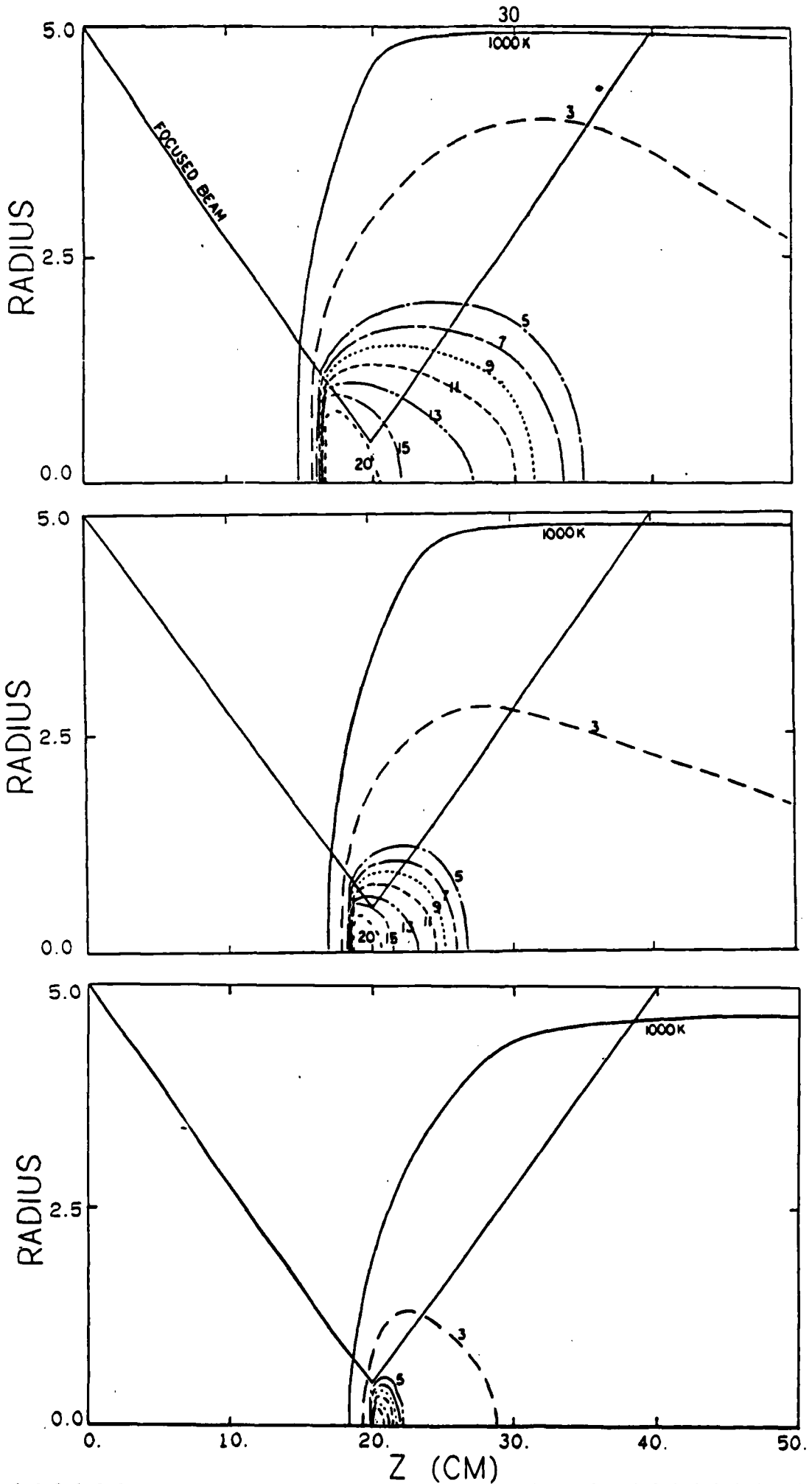


Figure 15 Predictions of Isotherms for Hydrogen at Variable Laser Power.

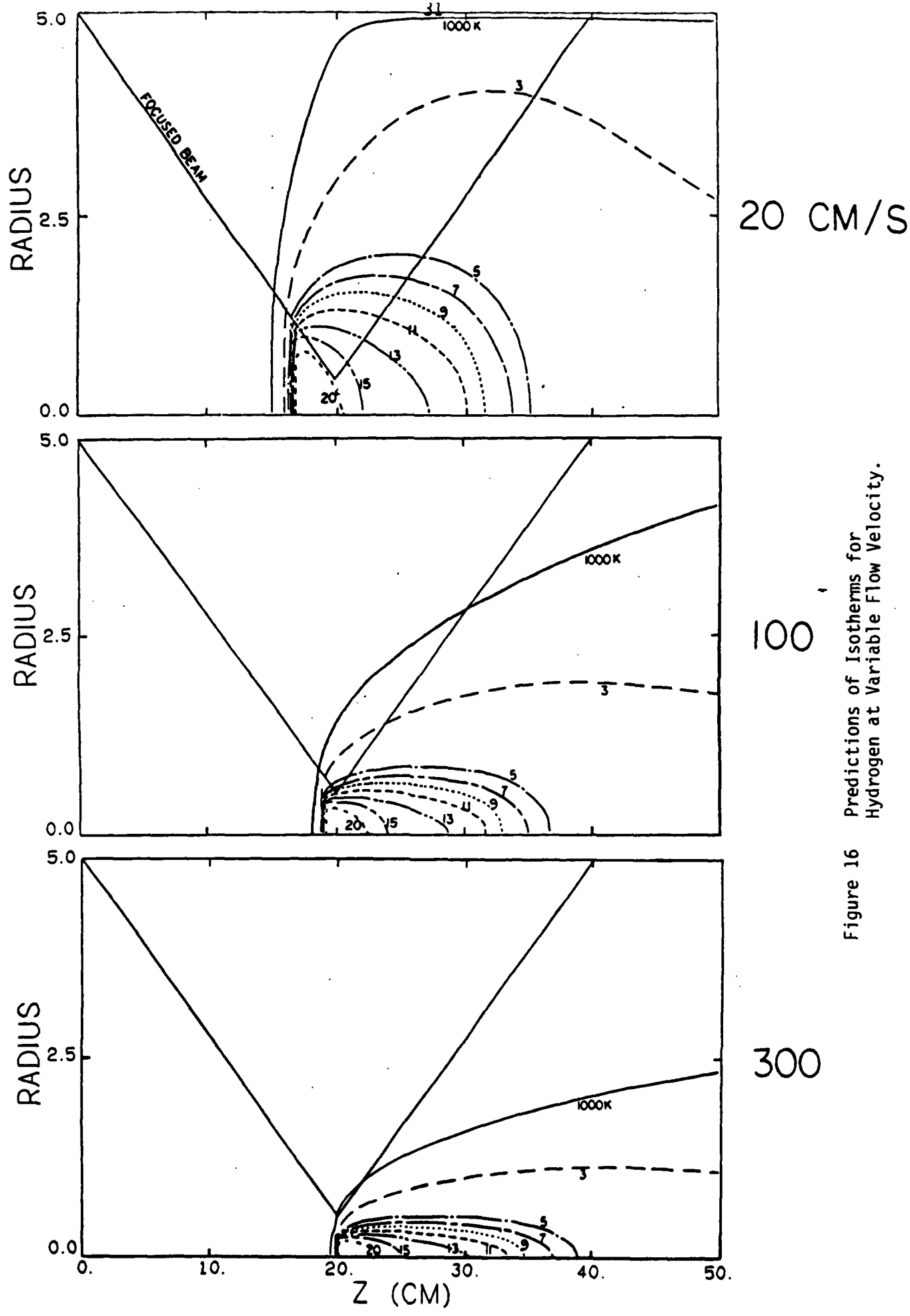


Figure 16 Predictions of Isotherms for Hydrogen at Variable Flow Velocity.

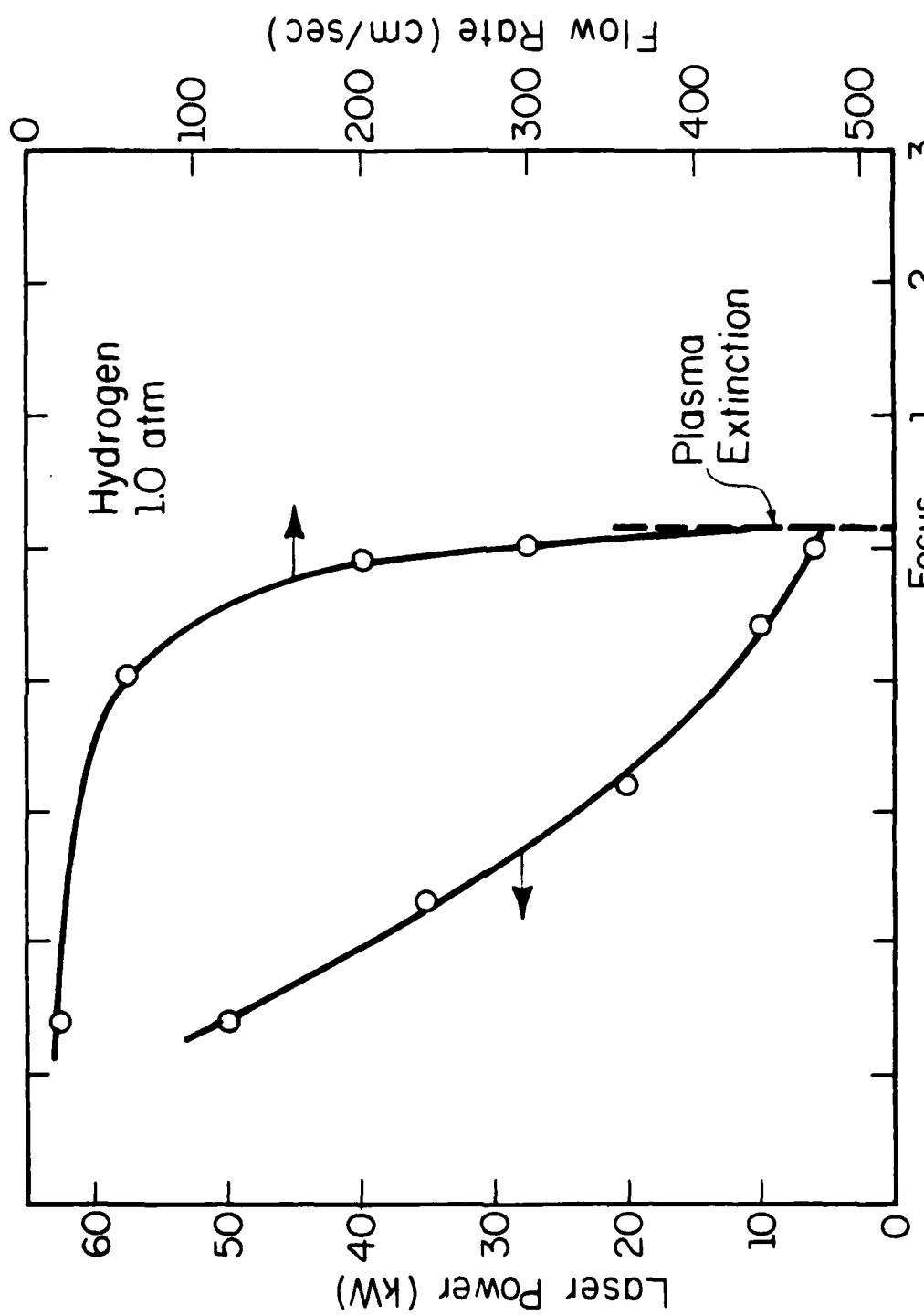


Figure 17 Plasma Front Location Versus Laser Power and Flow Velocity.

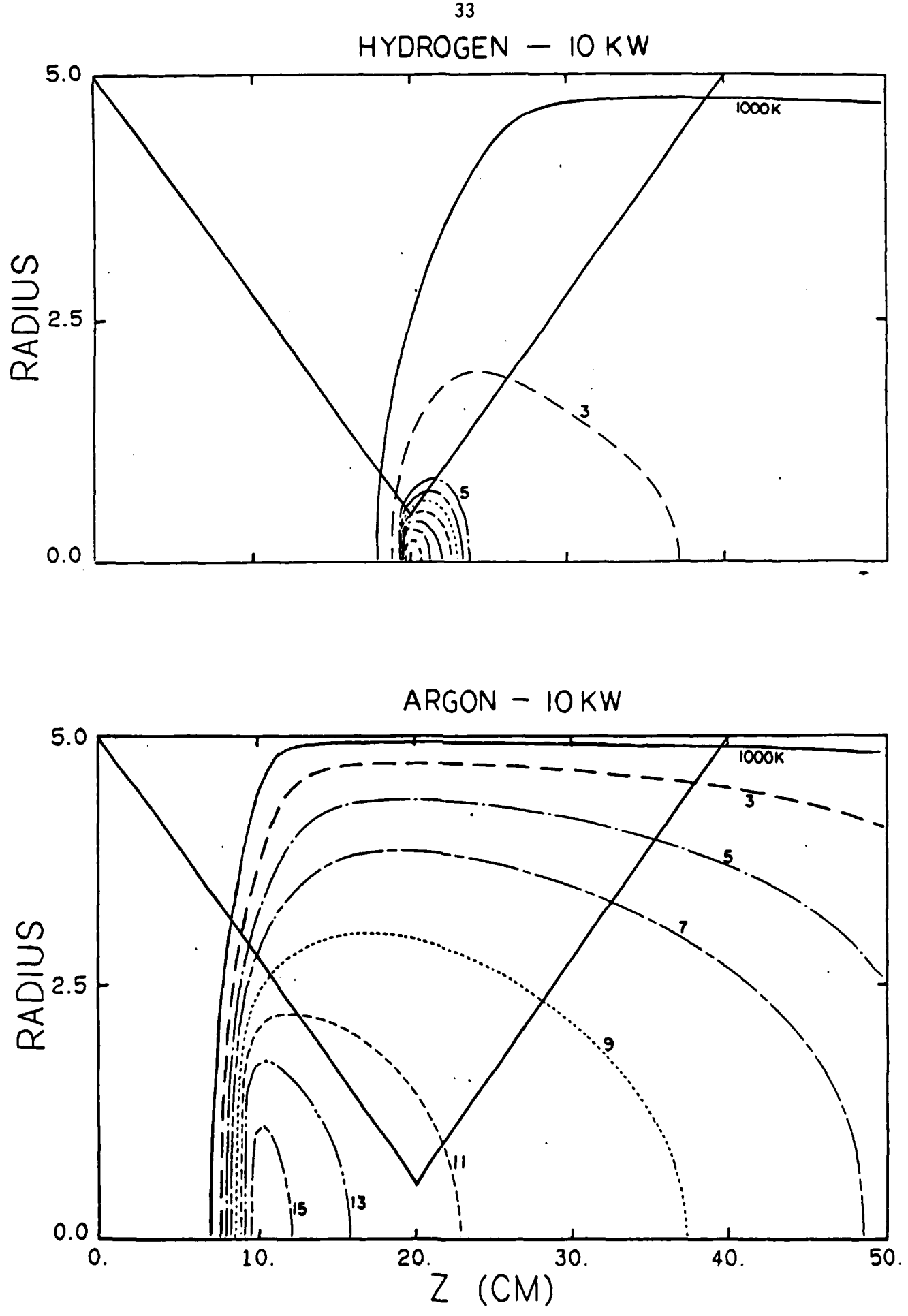


Figure 18 Comparison of Hydrogen and Argon Solutions at Identical Laser Power and Mass Flow Rate.

The argon plasmas observed in the laboratory are very similar in shape to these calculated solutions, but tend to be considerably smaller in size. When radiation losses are included in the model, the size of the plasma will fall dramatically.

Expected Status of Work (January 1986)

By the end of 1985, we plan to have completed the following objectives:

- Produce detailed temperature mappings of the plasma core using OMA-3 line emission scans
- Attempt to determine electron number densities using Stark broadening of hydrogen Balmer lines.
- Examine the emission characteristics of the argon plasma, determine which emission bands are important in radiative preheating and losses, and use these results in our heat addition model.
- Complete the calorimeter data by moving to higher pressures and flow rates.
- Measure the calorimeter correction factor using NaCl windows placed in front of the calorimeter.
- Extend thermocouple measurements closer to the plasma core, and include correction factors for radiative heating of the TC.
- Make detailed pitot static measurements of the PIFC flowfield.
- Use increased flow rates to study blowout behavior and higher Reynolds number regimes.
- Develop a firm understanding of the fluid mechanics and mixing behavior of the laser heat addition process.
- Test the IR filtering system to see if blooming is occurring; change filter material if necessary.
- Record additional IR images at higher pressures and flow rates.
- Fully automate the experimental procedure using the Fluke controller.
- Calibrate the 10 kW laser with a copper integrating sphere.

- Optimize the laser focal volume using a photon drag detector.
- Receive and install the excimer laser system.
- Design and install optics for the LIF system.
- Determine which seedant/transition combination is best suited for temperature measurements in the downstream flowfield.
- Use the heat addition model (with radiation losses now included) to produce a new set of isotherm maps at various laser powers and flow velocities.
- Include an approximate treatment of radial flow to account for the two-dimensionality of the flow.

Goals for 1986 and Beyond

- Implement LIF studies
- Attempt plasma initiation using UV excimer laser

# END

# FILMED

6-85

# DTIC